Materials Chemistry and Physics 281 (2022) 125899

Contents lists available at ScienceDirect

Materials Chemistry and Physics

journal homepage: www.elsevier.com/locate/matchemphys

Optoelectronic and electric properties of 8-Hydroxyquinoline-Based complexes with divalent metal ions

Ayhan Üngördü

Department of Chemistry, Faculty of Science, Sivas Cumhuriyet University, 58140, Sivas, Turkey

HIGHLIGHTS

- The complexes containing the 8-hydroxyquinoline were designed theoretically to investigate their optoelectronic properties.
- OLED tensors of studied molecules were calculated.
- The best candidates for optoelectronic devices were determined.
- Also, the electric properties were predicted with the help of NEGF-DFT technique.
- The best candidates for electronic devices were estimated.

GRAPHICAL ABSTRACT

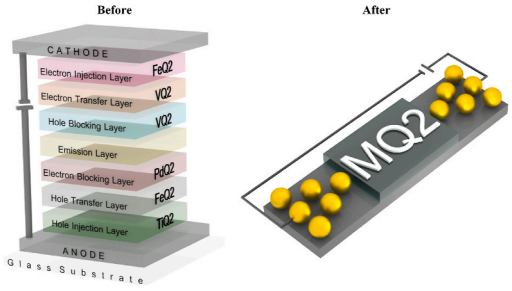

ARTICLE INFO

Keywords:
8-Hydroxyquinoline complexes
OLED material
Charge transfer rate
Electrical conductivity
NEGF technique

ABSTRACT

Firstly, the metallic complexes containing 8-hydroxyquinoline were designed theoretically to investigate their optoelectronic properties (M = Sc^{2+}, Ti^{2+}, V^{2+}, Cr^{2+}, Mn^{2+}, Fe^{2+}, Co^{2+}, Ni^{2+}, Cu^{2+}, Zn^{2+} Pd^{2+}, and Pt^{2+} and Q: 8-Hydroxyquinoline). Monomer calculations were executed at B3LYP/6-31G(d) level in Gaussian 16 program and LANL2DZ basis set was used only for Pd and Pt metals. On the other hand, dimer calculations were performed at B3LYP/TZP level by Amsterdam Density Functional (ADF) 2019 software. Using quantum chemical parameters, the optoelectronic behavior of the complexes was estimated and the best for devices such as the organic light emitting diode (OLED) structure was proposed. Secondly, the transport properties of the mentioned complexes are determined by nonequilibrium Green's function (NEGF) method based on the combination DFT in QuantumATK 2018 software. With this technique, the I–V characteristics and the transmission spectra of the investigated complexes is calculated and analyzed in range of 0–2 bias voltage. From the NEGF results, it is found that the best and the worst conductor complex in this voltage range and the best candidate for electronic devices like nanowires is suggested. The compounds studied in this study are considered as excellent candidates for next-generation optoelectronic and electronic devices.

1. Introduction

Display panels such as organic light emitting-diodes (OLEDs), light-emitting diodes (LEDs), and liquid crystal displays (LCDs) have extensively used during the past decades [1]. Among these, OLED panels have attracted great attention as they have some properties such as economic, efficient and flexible [2]. Some researchers working on OLED have focused on materials that affect OLED performance [3]. In the OLED structure, there are electron transfer layer (ETL), hole transfer layer (HTL), electron injection layer (EIL), hole injection layer (HIL), electron

E-mail address: aungordu@cumhuriyet.edu.tr.

https://doi.org/10.1016/j.matchemphys.2022.125899
Received 26 September 2021; Received in revised form 14 February 2022; Accepted 19 February 2022
Available online 22 February 2022
0254-0584/© 2022 Elsevier B.V. All rights reserved.

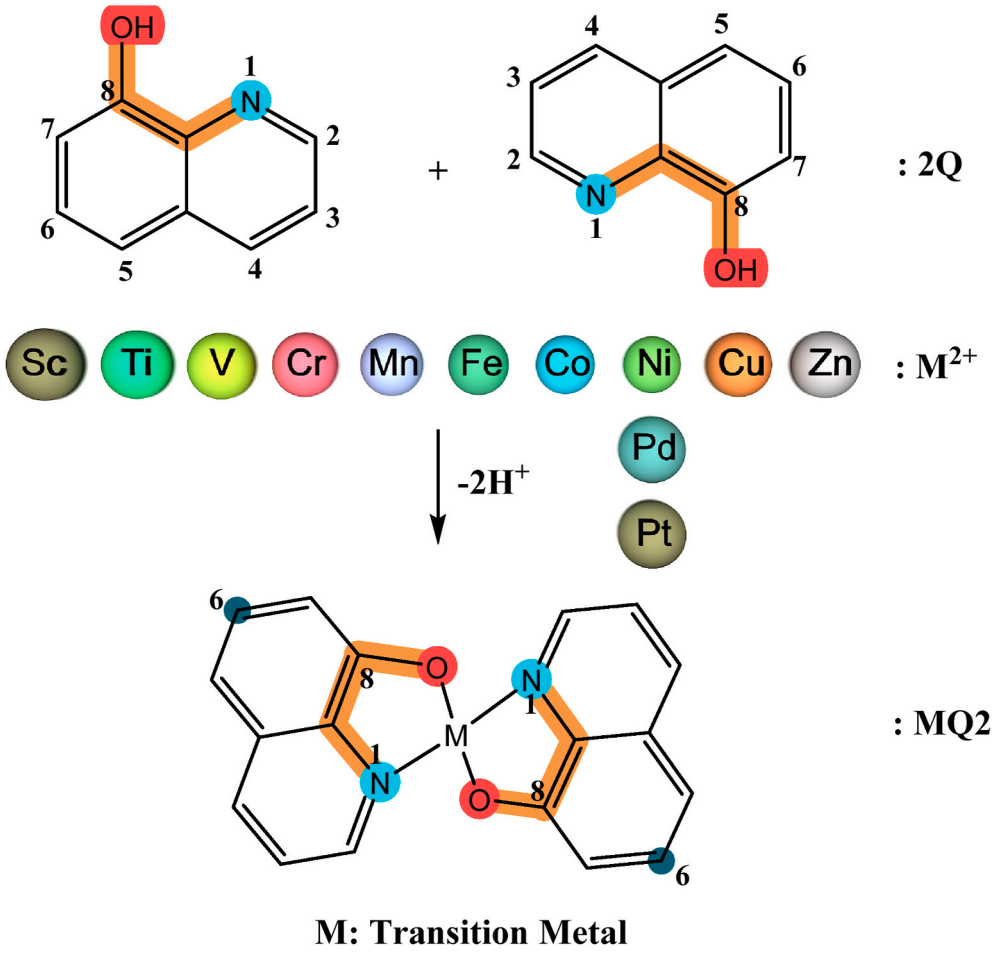

Fig. 1. The designed metal complexes containing 8-hydroxyquinoline ligand.

blocking layer (EBL), hole blocking layer (HBL) and emission layer (EL) between the cathode and anode [4]. To design a good OLED, it should be well done the select of molecules in the aforementioned layer. Standard HTL and an ETL compounds are N,N′-diphenyl-N,N′-bis(3-methlphenyl)-(1,10-biphenyl)-4,4′-diamine (TPD) and tris (8-hydroxyquinolinato)aluminum(III) (Alq3) molecules are respectively [5,6]. Researchers working to improve the performance of OLEDs have studied for the determination of alternative materials which are better than the two compounds mentioned [7,8]. The properties of the other materials described above, as well as ETL and HTL molecules, also undoubtedly affect the performance of OLED. Because of this, it is expected that a good selection of the materials mentioned in the OLED structure will lead to a good OLED design. Firstly, the presence of conjugated pi bonds in the chosen molecule is a good beginning [9]. Notably, the transition metal complexes including conjugated pi bonds are promising contenders as building blocks of optoelectronics [10].

In addition to opto-electronic properties of the compounds investigated, their electronic behaviors also are illuminated in the light of some important analyses on the *I–V* characteristics and the transmission spectra [11]. The prediction of the *conductivity properties* of the complexes provides important insights and clues about the design of electronic devices [12]. The materials with high conductivity are expected to be good circuit elements such as transistors and nanowires [13]. For that reason, the electronic properties of the examined compounds can be determined using computational chemistry tools [14].

Density Functional Theory (DFT) is a popular method used in computational chemistry tools [15]. There are many hybrid functions in the DFT method. B3LYP hybrid functional is one of the most extensively used functions as it has lower computational cost and more accuracy and it gives results compatible with experimental data [16]. Therefore, B3LYP function has widely been used in design studies [17]. Additionally, nonequilibrium Green's function (NEGF) technique is a well-known method for conductivity calculations. Generally, this technique is combined with DFT method [18].

In this paper, metal complexes consisting of 8-hydroxyquinoline ligand and all divalent first-row transition metals, palladium, and platin metals are designed by DFT method as seen in Fig. 1. Then optoelectronic behaviors of studied complexes are determined using quantum chemical descriptors such as the reorganization energy and the ionization potential. From the obtained data, it is suggested the suitable candidate/candidates for the layers in optoelectronic devices such as OLED structure. After that, the electronic properties of the studied complexes are estimated by the NEGF technique based on the DFT method. Among the investigated metal complexes, it is proposed that the best ones for electronic device elements like nanowires.

2. Methods

All calculations were executed in the vacuum with different computational chemistry software. Monomer calculations were carried out with the help of B3LYP functional using Gaussian 16 [19] and GaussView 6 [20] package programs and it was controlled that there are no imaginary frequencies in the lowest energy states. In the calculations, LANL2DZ basis set was considered for only Pd and Pt metals, while 6-31G(d) basis set was applied for the rest of the atoms. On the other hand, the calculations of dimer molecules were performed at B3LYP/TZP level via Amsterdam Density Functional (ADF) 2019 [21] program.

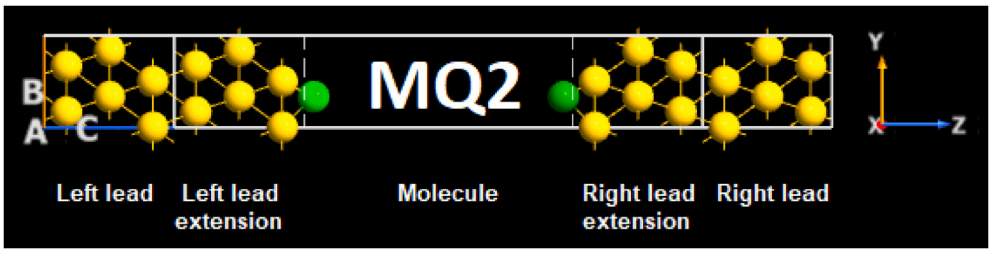

Fig. 2. Schematic description of MQ2 complexes between two bulk gold leads. (For interpretation of the references to colour in this figure legend, the reader is referred to the Web version of this article.)

To calculate charge transfer rate for electron or hole ($W_{e/h}$), Marcus-Hush equation [22,23] which is described by Eq. (1) can be used.

$$W_{e/h} = \frac{{V_{e/h}}^2}{\hbar}\left(\frac{\pi}{\lambda_{e/h} k_B T}\right)^{1/2} \exp\left(-\frac{\lambda_{e/h}}{4 k_B T}\right) \quad (1)$$

where T denotes the temperature, k_B and $\hbar$ denotes the Boltzmann constant and Dirac constant, respectively. $\lambda_{e(h)}$ and $V_{e(h)}$ stands for the electron (hole) reorganization energy and effective charge transfer integral for electron (hole), respectively. According to eq. (1), $W_{e/h}$ depend on $\lambda_{e(h)}$ and $V_{e(h)}$ at a constant temperature which is 298.15 K in the calculations. For high $W_{e(h)}$ values, $\lambda_{e(h)}$ and $V_{e(h)}$ need to be small and large, respectively.

The reorganization energies are significant parameters regarding the charge transfer in molecules. There are two types of reorganization energies (λ). These are called as the external and the internal reorganization energy which are abbreviated as λ_{ext} and λ_{int}, respectively.

The λ_{ext} is characterized by the result of polarize medium on charge transfer. In addition, the λ_{int} is owing to the structural alteration between ionic and neutral conditions. In the previous studies, it has been reported that there is a clear correlation between λint and W [24,25]. Accordingly, only the debate on λ_{int} is considered in the present article. The electron (λ_e) and hole (λ_h) reorganization energies of the molecules can be determined from the single point energy and they can be calculated by Eqs. (3) and (4) [26].

$$\lambda_e = \left(E_0^- - E_-^-\right) + \left(E_-^0 - E_0^0\right) \quad (2)$$

$$\lambda_h = \left(E_0^+ - E_+^+\right) + \left(E_+^0 - E_0^0\right) \quad (3)$$

The adiabatic and vertical ionization potentials (IP_a and IP_v) of the molecules can be computed from Eqs. (4) and (5), respectively. Their adiabatic and vertical electron affinities (EA_a and EA_v) are also calculated from Eqs. (6) and (7), respectively [27].

$$IPa = E_+^+ - E_0^0 \quad (4)$$

$$IPv = E_0^+ - E_0^0 \quad (5)$$

$$EAa = E_0^0 - E_-^- \quad (6)$$

$$EAv = E_0^0 - E_0^- \quad (7)$$

where $E_0^-(E_0^+)$ denotes the energy of the anion (cation) calculated by means of the optimized structure of the neutral compound. In the same way, $E_-^-(E_+^+)$ indicates the energy of the anion (cation) computed from the optimized anionic (cationic) state, $E_-^0(E_+^0)$ is the obtained energy of the neutral molecule calculated at the anion (cation) structure. Finally, E_0^0 means the calculated energy of the neutral compound at the ground state.

To predict the stability of compounds, the absolute hardness (η) can be calculated using adiabatic ionization potential (IPa) and electron affinity (EAa) via the following Eq. (8) [26].

$$\eta = (IPa - EAa)/2 \quad (8)$$

The electronic coupling ($V_{e/h}$) which are also known as effective (generalized) transfer integrals for hole transfer or electron transfer can be calculated using Eq. (9) [28].

$$V_{e/h} = \frac{J_{12} - S_{12}(E_1 + E_2)/2}{1 - {S_{12}}^2} \quad (9)$$

Here E_1 and E_2 are the site energies of monomer 1 and 2, respectively. J_{12} is the charge transfer integral, and S_{12} is the overlap integral. Additionally, J_{12}, S_{12}, E_1, and E_2 could be expressed as Eq. (10).

$$\begin{aligned} J_{12} &= \langle {\varphi_1}^{H/L} | h_{KS} | {\varphi_2}^{H/L} \rangle \\ S_{12} &= \langle {\varphi_1}^{H/L} | {\varphi_2}^{H/L} \rangle \\ E_1 &= \langle {\varphi_1}^{H/L} | h_{KS} | {\varphi_1}^{H/L} \rangle \\ E_2 &= \langle {\varphi_2}^{H/L} | h_{KS} | {\varphi_2}^{H/L} \rangle \end{aligned} \quad (10)$$

Where h_{KS} is the Kohn–Sham Hamiltonian of a dimer pair system and ${\varphi_1}^{H/L}$, ${\varphi_2}^{H/L}$ are the HOMOs or LUMOs of the two monomers [29]. For hole transport the highest occupied molecular orbitals (HOMOs) of monomers are used as the basis function while for electron transport the lowest unoccupied molecular orbitals (LUMOs) are used correspondingly.

In the calculation of electronic coupling, the fragment orbital approach is applied with Amsterdam density functional (ADF) software. Therefore, ADF program can be directly calculate the $V_{e/h}$ values of dimeric structures [30].

To investigate electron transport characteristics of mentioned complexes, each optimized complex was wired between two Au(111)-(2 × 2) electrodes through sulfur atom which was obtained by replacing the hydrogen atom in 6-position of the complex (ligand), as shown in Fig. 2. The distance between each electrode and the molecule was adjusted to be 1.71 Å. The value of 1.71 Å corresponds to an Au–S distance of 2.39 Å [31].

The electron transport features of MQ2 complexes were predicted by density functional theory (DFT) together with nonequilibrium Green's function (NEGF) method, as applied in QuantumATK 2018 program [32]. The exchange-correlation potential was defined by Perdew–Burke–Ernzerhof functional (PBE) of the generalized gradient approximation (GGA). The PseudoDojo pseudo-potentials and medium basis set were implemented, and wave functions of valence states were expanded as linear combination of atomic orbitals. A mesh cutoff of 125 Ryd and an electronic temperature of 300 K were adopted. The Brillouin zone was sampled with 6 × 6 × 134 k-point.

The current (I) was computed as a function of voltage from 0.0 to +2.0 V, and the transmission spectra were obtained in the region −2 to +2 eV with respect to the Fermi energy. When a bias voltage is implemented between the Left and Right electrodes, the electrons can transport across the molecule. The current passing through a molecular junction can be calculated from the probability of transmission (T(E,V)) as a function of the Landauer-Buttiker equation [33].

Table 1
The computed reorganization energies, adiabatic/vertical ionization potentials and adiabatic/vertical electron affinities, and absolute hardness values (all in eV) of MQ2 complexes B3LYP/6-31G(*d*)-LANL2DZ (Pd and Pt) level in the gas phase.

Complex	λe	λh	IPa	IPv	EAa	EAv	η
ScQ2	0.168	0.320	4.28	4.43	0.45	0.37	3.83
TiQ2	0.260	0.353	3.92	4.30	1.20	1.07	2.71
VQ2	0.080	0.935	5.35	5.87	0.23	0.14	5.12
CrQ2	0.223	0.258	4.13	4.28	2.15	2.04	1.98
MnQ2	0.237	0.522	6.15	6.78	0.88	0.76	5.27
FeQ2	0.248	0.068	5.09	5.13	1.92	1.79	3.17
CoQ2	0.228	0.343	6.76	0.17	0.26	0.14	6.51
NiQ2	0.161	0.114	6.22	6.27	0.56	0.48	5.66
CuQ2	1.550	0.676	6.79	7.11	0.90	0.20	5.89
ZnQ2	0.174	0.130	6.49	6.56	0.46	0.37	6.03
PdQ2	1.605	0.080	6.38	6.42	1.12	0.51	5.26
PtQ2	0.159	0.128	6.27	6.33	0.69	0.61	5.58

$$I=\frac{2e}{h}\int_{\mu_l}^{\mu_r} T(E,V)[(f(E-\mu_l)-f(E-\mu_r)]dE \quad (11)$$

where $\mu_{r(l)}$ denotes the chemical potential of right (left) electrode, $f(E-\mu_{r(l)})$ indicates the Fermi distribution function of electrons in the right (left) electrode, and T(E,V) shows the transmission coefficient at energy E and bias V, which can be achieved by the following equation:

$$T(E,V)=T_r\left[\Gamma_l(E)G^R(E)\Gamma_l(E)G^A(E)\right] \quad (12)$$

wherein, $G^R(E)$ and $G^A(E)$ are retarded and advanced Green's functions, respectively, the central scattering region, $\Gamma_{r(l)}=i[\sum_{r(l)}^{R}(E)-\sum_{r(l)}^{A}(E)]$ is the line width function, $\sum_{r(l)}^{R}(E)$ and $\sum_{r(l)}^{A}(E)$ are self-energies of the central scattering region, which include all the effect of the electrodes. The transmission coefficient T(E) can be decomposed into the contribution of n eigen channels:

$$T(E)=\sum_n T_n(E) \quad (13)$$

For the equilibrated system, the conductance G can be achieved by transmission function T(E) at the Fermi level E_F of the system.

$$G=G_0T(E_f)=G_0\sum T_n \quad (14)$$

Here $G_0 = 2e^2/h$ represents for the quantum unit of conductance. Lastly, h and e are the Planck constant and the electron charge, respectively.

3. RESULTS and DISCUSSION

3.1. The investigation of optoelectronic properties

3.1.1. Reorganization energies

According to the concept of reorganization energy, charge transfer rates of molecules can be predicted without electronic coupling ($V_{e/h}$) values [34,35]. However, more accurate values of charge transfer rates can be obtained via the calculation of V values [36]. The studies regarding reorganization energies refer to the Alq3 complex and TPD molecules as the standard ETL and HTL compounds, respectively [6,37]. The electron reorganization energy of Alq3 complex and the hole reorganization energy of TPD have reported as 0.276 eV and 0.290 eV, respectively [38,39]. Researchers studying on OLED materials have focused on finding molecules with lower reorganization energy than these values [40–42]. In other words, molecules having a lower reorganization energy show a higher OLED performance, as seen in Eq. (1). For that reason, the aforementioned reorganization energies of 8-hydroxyquinoline complexes in vacuum are computed at B3LYP/6-31G(d) level and given in Table 1.

Table 2
The calculated geometric parameters such as bond length (pm), bond angles (°) and dihedral angles (°) of MQ2 dimers B3LYP/TZP level in the gas phase.

Dimer	M1-M1′	N1-M1-N2	O1-M1-O2	N1-M1-M1′-N2′	O1-M1-M1′-O2′
ScQ2	313.1	90.7	159.8	190.7	137.3
TiQ2	297.5	155.6	158.1	175.4	191.6
VQ2	210.2	156.1	155.0	180.0	180.0
CrQ2	257.8	168.6	163.7	180.3	191.7
MnQ2	196.9	160.2	157.6	204.6	204.1
FeQ2	220.4	167.8	163.4	204.6	204.9
CoQ2	267.5	171.1	171.5	179.9	179.9
NiQ2	314.7	175.3	179.0	180.1	180.2
CuQ2	310.6	163.4	176.9	180.9	181.0
ZnQ2	295.5	113.3	154.6	283.9	171.3
PdQ2	313.6	176.4	177.8	180.0	180.0
PtQ2	307.3	175.5	176.7	180.0	180.0

Table 1 shows that electron reorganization energies of all complexes except for CuQ2 and PdQ2 are smaller than that of Alq3. It is noted that all mentioned complexes are better ETL materials than Alq3. Among them, Vq2 which have the lowest λe value (0.080 eV) is a perfect ETL candidate. Additionally, CuQ2 and PdQ2 complexes can be utilized as EBL molecules due to their high λe values [26,43]. On the other hand, as seen in Table 1, CrQ2, FeQ2, NiQ2, ZnQ2, PdQ2, and PtQ2 complexes are good HTL compounds because they have smaller λh values than that of TPD. Within them, Feq2 and PdQ2 molecules have small λh values. For that reason, they can be preferred as excellent HTL complex. In addition, VQ2 complex is a good candidate for HBL molecule owing to its high λh value [26,43].

3.1.2. Ionization potential, electron affinities and absolute hardness values

To predict the charge transfer facility of compounds in EIL and HIL layers, other important descriptors are the ionization potentials (IPs) and the electron affinities (EAs) that can be easily determined by computational chemistry tools. It is well-known that the lower the IP of molecule, the easier it is to create a hole [44]. Addition, the larger the EA of compound means better electron transport [45]. All adiabatic/vertical ionization potentials (IPa/IPv) and adiabatic/vertical electron affinities (EAa/EAv) of the mentioned complexes are calculated and given in Table 1. It is apparent from Table 1 that molecule with the lowest IP values and the highest EA values in the vacuum are TiQ2 and FeQ2 complexes, respectively. Therefore, it is said that TiQ2 molecule is a good HIL material and FeQ2 can be used as EIL molecule. On the other hand, it is known that chemical hardness (η) is a measure of the chemical stability and hard molecules are more stable compared to soft ones. Therefore, one can say that the stability is an important criterion to determine the nature of OLED materials. The chemical hardness values of studied complexes are obtained and presented in Table 1. From Table 1, it is seen that the η value (1.98 eV) of CrQ2 molecule is smallest among all mentioned compounds. For that reason, it can be said that this compound is unstable compared to other compounds.

3.1.3. Dimer geometries and effective (generalized) transfer integrals

To determine effective transfer integrals, $V_{e/h}$, researchers generally need to crystal data because it indicates the strength of the electronic coupling between the two adjacent neighboring compounds (dimer) [46,47]. Additionally, it has been reported that the charge transfer should be anisotropic [48]. In other words, the effective transfer integrals can be modified depending on the geometries of the dimers. Nevertheless, effective transfer integrals may be calculated for a particular geometry. Therefore, in the present article, it is taken into consideration that dimer geometries are almost parallel because the π-conjugated coupling interactions between the neighboring molecules are quite strong.

The optimized structures obtained at the LDA/DZ level using parallel geometry of two MQ2 complexes are shown in Fig. 1 and the geometric

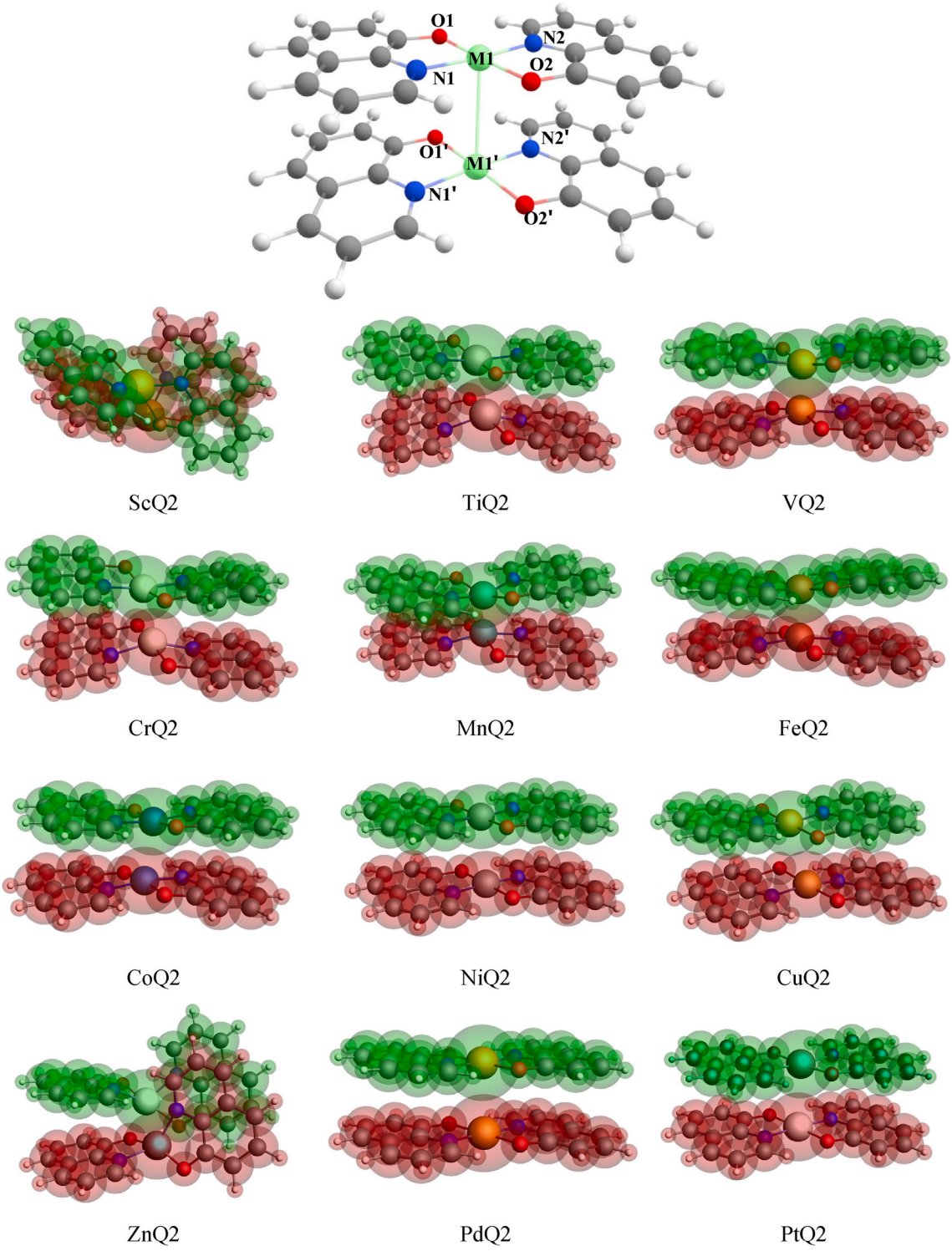

Fig. 3. The optimized structures of the mentioned dimers in vacuum.

parameters of these dimers are given in Table 2. As seen from dihedral angles in Table 2, while VQ2, CoQ2, NiQ2, CuQ2, PdQ2, and PtQ2 pairs are almost in the parallel-plane dimer, whereas other complexes are far from parallel-plane geometry.

The effective transfer integrals of dimer geometries shown in Fig. 3 are calculated at B3LYP/TZP level and the obtained results are tabulated in Table 3. It is well-known that the higher effective transfer integral is the larger charge transfer. Referring to Table 3., it is clear that absolute Ve values of ScQ2, VQ2, FeQ2, and CoQ2 are high. This shows that charge transfer of these molecules is large among all studied complex. On the other hand, it is apparent from the result given in Table 3 that absolute Vh values of VQ2, MnQ2, FeQ2, and CoQ2 are quite large and they have high hole transfer. As a result, one can said that VQ2, FeQ2, and CoQ2 complexes have high electron and hole transfer rates. For this reason, the three compounds can be used as ambipolar material.

3.1.4. Charge transfer rates

The charge transfer properties of the complexes can be quantitatively

Table 3
The obtained electron and hole transfer integrals (in eV) and the charge transfer rates (s^{-1}) of the mentioned molecules at B3LYP method in the gas phase.

Complex	V_e	V_h	W_e	W_h
ScQ2	−0.18887	0.14473	$2.85x10^{14}$	$2.77x10^{13}$
TiQ2	0.04261	0.00681	$4.77x10^{12}$	$4.23x10^{10}$
VQ2	−0.21696	−1.28533	$1.28x10^{15}$	$3.22x10^{12}$
CrQ2	−0.05222	0.12525	$1.11x10^{13}$	$4.22x10^{13}$
MnQ2	−0.12297	1.33678	$5.20x10^{13}$	$2.57x10^{14}$
FeQ2	0.91911	0.53269	$2.55x10^{15}$	$9.43x10^{15}$
CoQ2	−0.28117	−0.72795	$3.03x10^{14}$	$5.40x10^{14}$
NiQ2	0.01721	0.19711	$2.59x10^{12}$	$6.38x10^{14}$
CuQ2	0.01901	0.27121	$1.37x10^{6}$	$2.09x10^{12}$
ZnQ2	0.05272	0.06627	$2.06x10^{13}$	$5.78x10^{13}$
PdQ2	−0.00530	−0.00530	$2.52x10^{11}$	$3.05x10^{14}$
PtQ2	0.06221	−0.10613	$3.47x10^{13}$	$1.52x10^{14}$

determined by considering their charge transfer rates (W_e or W_h). To find the charge transfer rates, the values of all parameters (the reorganization energies, the transfer integrals, temperature, Boltzmann constant, etc.) appearing in the Marcus-Hush equation represented by Eq. (1) must be substituted into the equation. So, the electron and the hole transfer rates of the mentioned complexes can be predicted for given dimer geometry. In this way, the obtained $W_{e(h)}$ values of MQ2 complexes at 25 °C are tabulated in Table 3. Referring to Table 3., it is seen that all studied molecules except for W_e values of CuQ2 have relatively high electron and hole transfer rates. Among them, FeQ2 complex has the best electron transfer rate ($2.55x10^{15}$ s^{-1}) and hole transfer rate ($9.43x10^{15}$ s^{-1}). Consequently, it is said that FeQ2 molecule is the best candidate for both electron and hole transfer material because of its high charge rates.

3.2. The investigation of electrical properties

3.2.1. Current-volt plots

NEGF-DFT technique have been used to predict the electronic features of the compounds. The molecular junctions with molecules between gold electrodes are given in Figs. S1–S12. The voltages in the range of 0–2 V were applied to the mentioned devices. The obtained

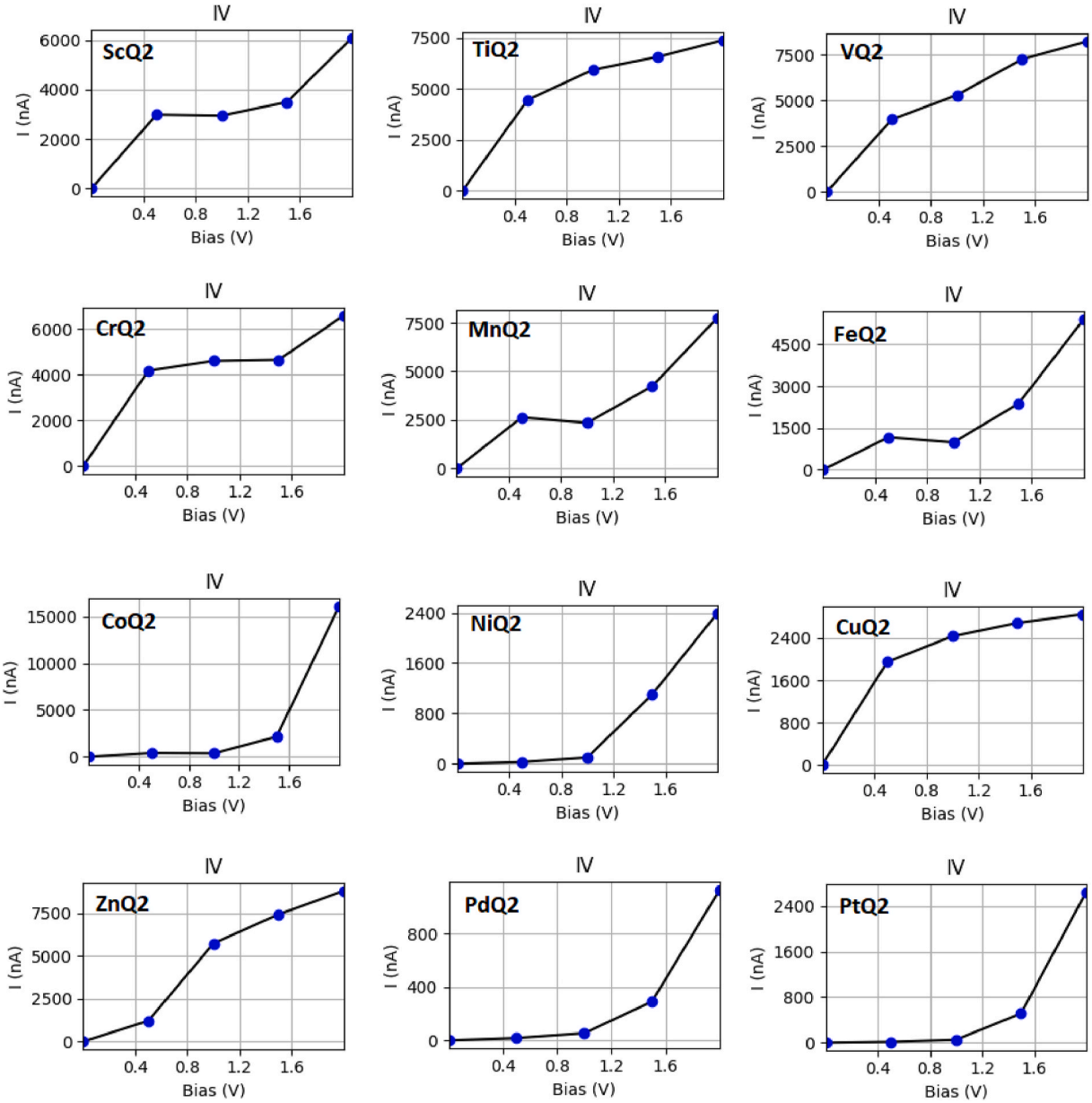

Fig. 4. The I–V curves of the device with MQ2 complexes.

current-voltage plots are shown in Fig. 4.

Referring to Fig. 2, it is seen that the current values of almost all complex increase with applied voltage. The maximum current for every complex is obtained at 2 V. In the mentioned complexes, the highest current (16,134 nA) at 2 V is acquired from the CoQ2 molecule. However, the current values of the Co-complex are relatively low under the 2 V. The current values of ScQ2, TiQ2, VQ2, CrQ2, and MnQ2 compounds in the range of 0.5 V–1.5 V are over 2000 nA. According to this, it can be said that the electrical conductivities of ScQ2, TiQ2, VQ2, CrQ2, and MnQ2 complexes are good. On the other hand, it is clearly shown that from Fig. 4 that the electrical conductance of NiQ2, CuQ2, PdQ2, and PtQ2 compounds are quite low in the applied voltages. Among them, Pd-complex is the worst conductor.

Additionally, it is indicated that the current values of VQ2 and ZnQ2 molecules at 1.5 V are 7268 nA and 7443 nA, respectively. The current values are higher than that of CoQ2 at the same bias. For that reason, it can be stated that VQ2 and ZnQ2 complexes are more conductor than CoQ2 at 1.5 V.

In the light of NEGF results, the materials for circuit elements such as transistors and nanowires can be roughly predicted in the range of 0–2 V. At 2 V, the best material for nano-devices is CoQ2 complex in the investigated compounds. For a similar purpose, ScQ2, TiQ2, VQ2, CrQ2, MnQ2 FeQ2, CuQ2, and ZnQ2 complexes can be used under 2 V. Additionally, it can be said that NiQ2, PdQ2, and PtQ2 molecules is not good materials below 2 V.

3.2.2. *Transmission spectra*

In order to obtain detailed information on I–V plots, it is necessary to carry out research on transmission spectra. The transmission spectra for the aforementioned nano-constructed with MQ2 complexes are calculated at the bias voltage of 0.0, 0.5, 1.0, 1.5 and 2.0 V and the achieved spectra are presented in Supplementary Information (Figs. S13–S24).

At a 0.0 V bias, the electrons can be transmitted through a molecular junction through a nonresonant tunnel. The implementation of a certain bias alters the position of the occupied and unoccupied molecular orbitals relative to the Fermi level. This allows the transport of electrons through a molecular junction by using the orbitals mentioned as the dominant transport channel. In addition, molecular orbitals with energy close to the Fermi level contribute to the current and give peaks near the Fermi energy in the bias window of the transmission spectra [49]. The bias windows in transmission spectra are areas between dotted lines in Figs. S13–S24.

From Figs. S13–S24., it is clearly seen that the increasing the number of the peaks in the bias windows increases the current. It should be also taken into account that current intensity increases with the transmission coefficient. Among the aforementioned transmission spectra at 2V, it is clear that the molecular junction with CoQ2 compound has the most peak number and the highest transmission coefficient in the bias window. Therefore, it can be said that CoQ2 has the highest conductivity at 2 V. On the other hand, it is obvious that there are almost no peaks in the transmission spectra of the device with PdQ2 complex. This indicates that the Pt-complex has low conductivity.

4. Conclusions

In first section of the present article, the OLED behaviors of the transition metal complex containing the 8-hydroxyquinoline (MQ2) are investigated by using quantum chemical parameters such as reorganization energy, ionization potential and electron affinity. The reorganization energies determine that VQ2 and FeQ2 are excellent candidates for electron and hole transfer materials, respectively. Furthermore, these parameters determine that the best electron and hole blocking molecules are PdQ2 and VQ2 compounds, respectively. By means of the ionization potentials and electron affinities, it is stated that TiQ2 and FeQ2 can be used to be hole injection and electron injection molecules, respectively. From the effective transfer integrals, it is clear that VQ2, FeQ2, and CoQ2 complexes have high electron and hole transfer ratios in the given parallel geometry. Finally, it should be noted that the FeQ2 complex among the molecules mentioned in the given dimer geometries have the highest transfer rates of electrons and holes.

In the second part of the article, the electrical properties of the mentioned MQ2 complexes are examined by the NEGF method. The NEGF technique provides detailed information about the electrical conductivities of the investigated molecules. With this method, it is found that the electrical conductivities of ScQ2, TiQ2, VQ2, CrQ2, and MnQ2 complexes are quite good in the range of 0–2 V. Additionally, it should be emphasized that the CoQ2 molecule has the highest conductivity at 2 V. On the other hand, it can be stated that the electrical conductance of NiQ2, CuQ2, PdQ2, and PtQ2 compounds are quite low in the applied voltages. Among them, it should be said that the conductivity of Pd-complex is very low.

Declaration of competing interest

The authors declare that they have no known competing financial interests or personal relationships that could have appeared to influence the work reported in this paper.

Acknowledgements

The numerical calculations reported in this paper were fully/partially performed at TUBITAK ULAKBIM, High Performance and Grid Computing Center (TRUBA resources).

Appendix A. Supplementary data

Supplementary data to this article can be found online at https://doi.org/10.1016/j.matchemphys.2022.125899.

References

[1] Z.F. He, Y. Liu, Z.L. Yang, J. Li, J.Y. Cui, D. Chen, Z.S. Fang, H.P. He, Z.Z. Ye, H. M. Zhu, N.N. Wang, J.P. Wang, Y.Z. Jin, High-efficiency red light-emitting diodes based on multiple quantum wells of phenylbutylammonium-cesium lead iodide perovskites, ACS Photonics 6 (3) (2019) 587–594.
[2] R.E. Triambulo, J.H. Kim, J.W. Park, Highly flexible organic light-emitting diodes on patterned Ag nanowire network transparent electrodes, Org. Electron. 71 (2019) 220–226.
[3] S. Negi, P. Mittal, B. Kumar, Impact of different layers on performance of OLED, Microsyst. Technol. 24 (12) (2018) 4981–4989.
[4] R.B. Choudhary, R. Kandulna, 2-D rGO impregnated circular-tetragonal-bipyramidal structure of PPY-TiO2-rGO nanocomposite as ETL for OLED and supercapacitor electrode materials, Mater. Sci. Semicond. Process. 94 (2019) 86–96.
[5] H.H. Horhold, H. Tillmann, D. Raabe, M. Helbig, W. Elflein, A. Brauer, W. Holzer, A. Penzkofer, Synthesis of TPD-containing polymers for use as light emitting materials in electroluminescent and Laser devices, Org. Light-Emitt. Mater. Dev. Iv 4105 (2000) 431–442.
[6] A. Yamamori, C. Adachi, T. Koyama, Y. Taniguchi, Electroluminescence of organic light emitting diodes with a thick hole transport layer composed of a triphenylamine based polymer doped with an antimonium compound, J. Appl. Phys. 86 (8) (1999) 4369–4376.
[7] F. de Jong, M. Daniels, L. Vega-Castillo, K. Kennes, C. Martin, G. de Miguel, M. Cano, M. Perez-Morales, J. Hofkens, W. Dehaen, M. Van der Auweraer, 5,10-Dihydrobenzo[a]indolo[2,3-c]carbazoles as Novel OLED Emitters, J. Phys. Chem. B 123 (6) (2019) 1400–1411.
[8] D.M. Han, P. Gong, S.H. Lv, L.H. Zhao, H.N. Zhao, DFT/TDDFT investigation on the photophysical properties of a series of phosphorescent cyclometalated complexes based on the benchmark complex FIrpic, Mol. Phys. 116 (9) (2018) 1218–1226.
[9] Q. Wei, Z.Y. Ge, B. Voit, Thermally activated delayed fluorescent polymers: structures, properties, and applications in OLED devices, Macromol. Rapid Commun. 40 (1) (2019).
[10] N. Altinolcek, A. Battal, M. Tavasli, J. Cameron, W.J. Peveler, H.A. Yu, P. J. Skabara, Yellowish-orange and red emitting quinoline-based iridium(III) complexes: synthesis, thermal, optical and electrochemical properties and OLED application, Synthetic Met. 268 (2020).
[11] Y.S. Yang, M. Zhou, Y.X. Xing, Symmetry-dependent transport properties of gamma-Graphyne-based molecular magnetic tunnel junctions, Acta Phys. Chim. Sin. 38 (4) (2022).
[12] D. Sergeyev, N. Ashikov, N. Zhanturina, Electric transport properties of a model nanojunction "Graphene-Fullerene C-60-Graphene, Int. J. Nanosci. 20 (1) (2021).

[13] R.R. Thakur, N. Chaturvedi, Design, optimization, and analysis of Si and GaN nanowire FETs for 3 nm technology, Semicond. Sci. Technol. 36 (7) (2021).
[14] E.P. Hoy, D.A. Mazziotti, T. Seideman, Development and application of a 2-electron reduced density matrix approach to electron transport via molecular junctions, J. Chem. Phys. 147 (18) (2017).
[15] S. Kaya, P. Banerjee, S.K. Saha, B. Tuzun, C. Kaya, Theoretical evaluation of some benzotriazole and phospono derivatives as aluminum corrosion inhibitors: DFT and molecular dynamics simulation approaches, RSC Adv. 6 (78) (2016) 74550–74559.
[16] S. Kaya, C. Kaya, L. Guo, F. Kandemirli, B. Tuzun, I. Ugurlu, L.H. Madkour, M. Saracoglu, Quantum chemical and molecular dynamics simulation studies on inhibition performances of some thiazole and thiadiazole derivatives against corrosion of iron, J. Mol. Liq. 219 (2016) 497–504.
[17] M.H. Xiao, X.H. Jin, J.H. Zhou, B.C. Hu, Molecular design and selection of 1,2,5-oxadiazole derivatives as high-energy-density materials, New J. Chem. 43 (29) (2019) 11610–11617.
[18] D.F.S. Ferreira, W.D. Oliveira, E. Belo, R. Gester, M.R.S. Siqueira, A.M.J.C. Neto, J. Del Nero, Electron scattering processes in steroid molecules via NEGF-DFT: the opening of conduction channels by central oxygen, J. Mol. Graph. Model. 101 (2020).
[19] M.J. Frisch, G.W. Trucks, H.B. Schlegel, G.E. Scuseria, M.A. Robb, J.R. Cheeseman, G. Scalmani, V. Barone, G.A. Petersson, H. Nakatsuji, X. Li, M. Caricato, A. V. Marenich, J. Bloino, B.G. Janesko, R. Gomperts, B. Mennucci, H.P. Hratchian, J. V. Ortiz, A.F. Izmaylov, J.L. Sonnenberg, Williams, F. Ding, F. Lipparini, F. Egidi, J. Goings, B. Peng, A. Petrone, T. Henderson, D. Ranasinghe, V.G. Zakrzewski, J. Gao, N. Rega, G. Zheng, W. Liang, M. Hada, M. Ehara, K. Toyota, R. Fukuda, J. Hasegawa, M. Ishida, T. Nakajima, Y. Honda, O. Kitao, H. Nakai, T. Vreven, K. Throssell, J.A. Montgomery Jr., J.E. Peralta, F. Ogliaro, M.J. Bearpark, J. J. Heyd, E.N. Brothers, K.N. Kudin, V.N. Staroverov, T.A. Keith, R. Kobayashi, J. Normand, K. Raghavachari, A.P. Rendell, J.C. Burant, S.S. Iyengar, J. Tomasi, M. Cossi, J.M. Millam, M. Klene, C. Adamo, R. Cammi, J.W. Ochterski, R.L. Martin, K. Morokuma, O. Farkas, J.B. Foresman, D.J. Fox, Gaussian 16, Rev. B.01, Wallingford, CT, 2016.
[20] R. Dennington, T.A. Keith, J.M. Millam, GaussView, Version 6, Semichem Inc., Shawnee Mission, KS, 2016.
[21] S.C.M. Adf2019, Theoretical chemistry, Vrije Universiteit, Amsterdam, The Netherlands, http://www.scm.com.
[22] N.S. Hush, Adiabatic rate processes at electrodes. I. Energy-Charge relationships, J. Chem. Phys. 28 (1958) 962–972.
[23] R.A. Marcus, Electron-transfer reactions in chemistry - theory and experiment, Rev. Mod. Phys. 65 (3) (1993) 599–610.
[24] M.E. Kose, H. Long, K. Kim, P. Graf, D. Ginley, Charge transport simulations in conjugated dendrimers, J. Phys. Chem. 114 (12) (2010) 4388–4393.
[25] G.R. Hutchison, M.A. Ratner, T.J. Marks, Hopping transport in conductive heterocyclic oligomers: reorganization energies and substituent effects, J. Am. Chem. Soc. 127 (7) (2005) 2339–2350.
[26] U. Daswani, U. Singh, P. Sharma, A. Kumar, From molecules to devices: a DFT/TD-DFT study of dipole moment and internal reorganization energies in optoelectronically active aryl azo chromophores, J. Phys. Chem. C 122 (26) (2018) 14390–14401.
[27] A. Irfan, A. Kalam, A.R. Chaudhry, A.G. Al-Sehemi, S. Muhammad, Electro-optical, nonlinear and charge transfer properties of naphthalene based compounds: a dual approach study, Optik 132 (2017) 101–110.
[28] E.F. Valeev, V. Coropceanu, D.A. da Silva Filho, S. Salman, J.-L. Brédas, Effect of electronic polarization on charge-transport parameters in molecular organic semiconductors, J. Am. Chem. Soc. 128 (30) (2006) 9882–9886.
[29] X. Zhang, A.P. Côté, A.J. Matzger, Synthesis and structure of fused α-oligothiophenes with up to seven rings, J. Am. Chem. Soc. 127 (30) (2005) 10502–10503.
[30] W.Q. Deng, L. Sun, J.D. Huang, S. Chai, S.H. Wen, K.L. Han, Quantitative prediction of charge mobilities of pi-stacked systems by first-principles simulation, Nat. Protoc. 10 (4) (2015) 632–642.
[31] K. Stokbro, J. Taylor, M. Brandbyge, J.-L. Mozos, P. Ordejon, Theoretical study of the nonlinear conductance of Di-thiol benzene coupled to Au (1 1 1) surfaces via thiol and thiolate bonds, Comput. Mater. Sci. 27 (1–2) (2003) 151–160.
[32] S. Smidstrup, T. Markussen, P. Vancraeyveld, J. Wellendorff, J. Schneider, T. Gunst, B. Verstichel, D. Stradi, P.A. Khomyakov, U.G. Vej-Hansen, QuantumATK: an integrated platform of electronic and atomic-scale modelling tools, J. Phys. Condens. Matter 32 (1) (2019), 015901.
[33] M. Buttiker, Y. Imry, R. Landauer, S. Pinhas, Generalized many-channel conductance formula with application to small rings, Phys. Rev. B 31 (10) (1985) 6207–6215.
[34] A. Chakraborty, G.N. Reddy, M. Jana, S. Giri, [8] Cyclo-1, 4-naphthylene: a possible new member in hole transport family, Chem. Phys. Lett. 715 (2019) 153–159.
[35] T. Sutradhar, A. Misra, Role of electron-donating and electron-withdrawing groups in tuning the optoelectronic properties of difluoroboron-napthyridine analogues, J. Phys. Chem. 122 (16) (2018) 4111–4120.
[36] J. Ajantha, E. Varathan, V. Bharti, V. Subramanian, S. Easwaramoorthi, S. Chand, Photophysical and charge transport properties of pyrazolines, RSC Adv. 6 (1) (2016) 786–795.
[37] R. Reyes, E.N. Hering, M. Cremona, C.F.B. da Silva, H.F. Brito, C.A. Achete, Growth and characterization of OLED with samarium complex as emitting and electron transporting layer, Thin Solid Films 420 (2002) 23–29.
[38] N.E. Gruhn, D.A. da Silva, T.G. Bill, M. Malagoli, V. Coropceanu, A. Kahn, J. L. Bredas, The vibrational reorganization energy in pentacene: molecular influences on charge transport, J. Am. Chem. Soc. 124 (27) (2002) 7918–7919.
[39] A. Lukyanov, C. Lennartz, D. Andrienko, Amorphous films of tris(8-hydroxyquinolinato)aluminium: force-field, morphology, and charge transport, Phys. Status Solidi 206 (12) (2009) 2737–2742.
[40] J.L. Rao, K. Bhanuprakash, Push-pull effect on the geometrical, optical and charge transfer properties of disubstituted derivatives of mer-tris(4-hydroxy-1,5-naphthyridinato) aluminum (mer-AlND3), Open Chem. 14 (1) (2016) 20–32.
[41] A. Irfan, R.H. Cui, J.P. Zhang, L.Z. Hao, Push-pull effect on the charge transfer, and tuning of emitting color for disubstituted derivatives of mer-Alq3, Chem. Phys. 364 (1–3) (2009) 39–45.
[42] L.L. Shi, B. Hong, W. Guan, Z.J. Wu, Z.M. Su, DFT/TD-DFT study on the electronic structures and optoelectronic properties of several blue-emitting iridium(III) complexes, J. Phys. Chem. 114 (24) (2010) 6559–6564.
[43] S. Jang, S.H. Han, J.Y. Lee, Y. Lee, Pyrimidine based hole-blocking materials with high triplet energy and glass transition temperature for blue phosphorescent OLEDs, Synthetic Met. 239 (2018) 43–50.
[44] R.K. Chan, S.C. Liao, Dipole moments, charge-transfer parameters, and ionization potentials of methyl-substituted benzene-tetracyanoethylene complexes, Can. J. Chem. 48 (2) (1970) 299–&.
[45] A.A. Youssef, S.M. Bouzzine, Z.M.E. Fahim, I. Sidir, M. Hamidi, M. Bouachrine, Designing Donor-Acceptor thienopyrazine derivatives for more efficient organic photovoltaic solar cell: a DFT study, Physica B 560 (2019) 111–125.
[46] X.D. Yang, L.J. Wang, C.L. Wang, W. Long, Z.G. Shuai, Influences of crystal structures and molecular sizes on the charge mobility of organic semiconductors: Oligothiophenes, Chem. Mater. 20 (9) (2008) 3205–3211.
[47] C.L. Wang, F.H. Wang, X.D. Yang, Q.K. Li, Z.G. Shuai, Theoretical comparative studies of charge mobilities for molecular materials: pet versus bnpery, Org. Electron. 9 (5) (2008) 635–640.
[48] G.H. Meng, Y.P. Feng, X.D. Song, Y.T. Shi, M. Ji, Y. Xue, C. Hao, Theoretical insight into the carrier mobility anisotropy of organic-inorganic perovskite CH3NH3PbI3, J. Electroanal. Chem. 810 (2018) 11–17.
[49] A.M. El-Nahas, A. Staykov, K. Yoshizawa, Electrical conductance and diode-like behavior of substituted azulene, J. Phys. Chem. C 121 (5) (2017) 2504–2511.

MATERIALS CHEMISTRY AND PHYSICS

PublisherName: ELSEVIER SCIENCE SA

Journal Impact Factor ™

2021	Five Year
4.778	4.233

JCR Category	Category Rank	Category Quartile
MATERIALS SCIENCE, MULTIDISCIPLINARY *in SCIE edition*	125/345	Q2

Source: Journal Citation Reports 2021. Learn more

Journal Citation Indicator ™

2021	2020
0.86	0.76

JCI Category	Category Rank	Category Quartile
MATERIALS SCIENCE, MULTIDISCIPLINARY *in SCIE edition*	117/414	Q2

The Journal Citation Indicator is a measure of the average Category Normalized Citation Impact (CNCI) of citable items (articles and reviews) published by a journal over a recent three year period. It is used to help you evaluate journals based on other metrics besides the Journal Impact Factor (JIF).

Learn more